17th World Conference on Earthquake Engineering, 17WCEE
Sendai, Japan - September 13th to 18th 2020

RESISTANCE MECHANISM OF THE SLOPED CEILING COMPOSED WITH BRACES AND COMPRESSION-REINFORCED HANGING RODS

R. Morohoshi [1], F. Sakuraba [2], K. Yamazato [3], K. Suzuki [4] , T. Hanzawa [5], K. Harayama [6], T. Masato [7], S. Motoyui [8]

[1] *Engineer, Shimizu Corporation, r.sakanaka@shimz.co.jp*
[2] *Manager&Senior research engineer, Shimizu Corporation, f.sakuraba@shimz.co.jp*
[3] *Engineer, Shimizu Corporation, yamazato@shimz.co.jp*
[4] *Senior research engineer, Shimizu Corporation, suzuki.kenji@shimz.co.jp*
[5] *Manager&Senior research engineer, Shimizu Corporation, hanzawa_t@shimz.co.jp*
[6] *Manager, Shimizu Corporation, harayama@shimz.co.jp*
[7] *Senior engineer, Shimizu Corporation, t.masato@shimz.co.jp*
[8] *Professor, Tokyo Institute of Technology, motoyui.s.aa@m.titech.ac.jp*

Abstract

A seismic engineering for main structure of building has been improved through the experiences of huge structural damage by major earthquakes. On the other hand, the evaluation of non-structural components has not been caught up enough. In The 2011 off the Pacific coast of Tohoku Earthquake, we had a number of considerable seismic damages of non-structural elements, especially for suspended ceilings, about 2,000 damages with various level were reported. From the lessons of these cases, it has become in great focus that human injuries by ceiling collapse are big problem. Ceilings with various shapes are designed for aesthetic reason. The sloped ceiling tends to be applied for large scale facilities like concert halls and theaters. Having limited knowledge and experimental results, appropriate seismic design method for sloped ceiling is not established well. Therefore, the theoretical study on the static and dynamic behavior of the whole system of the sloped ceiling is essential for appropriate ceiling design.

In general, diagonal braces are arranged mainly to resist horizontal force by an earthquake. It is observed in previous tests of horizontal ceiling with braces that horizontal force causes the excitation mainly in horizontal direction and very slightly in vertical direction. On the other hand, in case of the sloped ceiling, as the interaction between horizontal response and vertical one is more noticeable due to the geometric feature, the vertical component cannot be ignored. In other words, in-plane and out-of-plane behavior of the sloped ceiling surface influence each other. Therefore, we have to consider the interaction between the horizontal and the vertical component carefully.

The purpose of this paper is to clarify the static and dynamic behavior of the sloped ceiling experimentally and numerically. Fig.1 shows a test specimen used in a shaking table test and Fig.2 shows examples of experimental results. As shown in Fig.2(a), out-of-plane response acceleration were also occured in the same magnitude as in-plane one though only the horizontal acceleration were input. And Fig.2(b) & (c) show axial forces on braces and a hanging rod. It is significant that the axial force on the hanging rod varies stable and its negative value(compressive value) is considerable. The phenomenon is the typical characteristics of the seismic resistance mechanism in the sloped ceiling subjected to horizontal acceleration. Through these experimental results and other numerical results, we suggest a new ceiling system composed with the braces developed previously and the hanging rods which can resist compressive axial force like a “Buckling Restrained Brace”. We sure that the combination of braces and hanging rods can improve the seismic performance of the sloped ceiling.

Keywords: sloped ceiling, horizontal and vertical behavior, hanging rod, dynamic experiment, numerical analysis

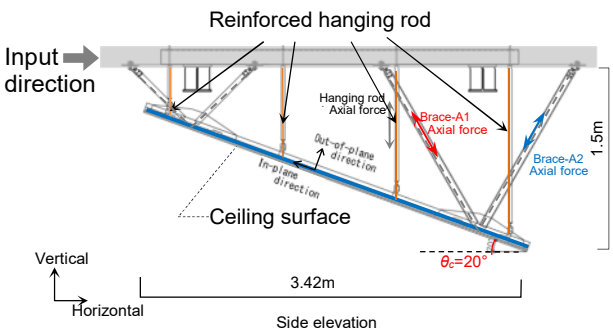

Figure 1 Experimental model

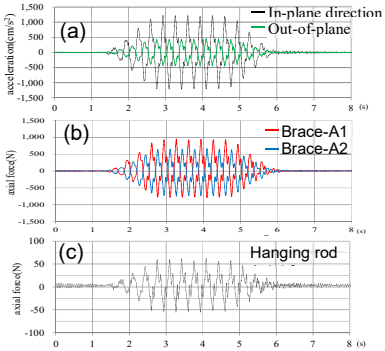

Figure 2 Experimental results

1. Introduction

Lessons learned from major earthquakes in the past have led to great improvements in the seismic engineering of the main structure of buildings. On the other hand, the evaluation of non-structural components has lagged behind. In the 2011 Off the Pacific Coast of Tohoku Earthquake, many cases of seismic damage to non-structural elements were reported, with suspended ceilings alone accounting for about 2,000 reports of damage to varying degrees. Photos1 (a) to (c) show the damages of ceilings during the 2011 earthquake in japan. Learning from these cases, it has become apparent that human injury caused by ceiling collapse is a serious problem. The most commonly affected types of facility where ceiling damage occured were sports arenas, assembly areas like entrance halls and concourses, exhibition halls, and similar. Ceilings in these facilities are large and have various forms, with sloped designs very common. The behavior of those ceilings is more complex than that of flat designs. With the collapse of such a ceiling, the affected space becomes unavailable for continued use but also for evacuation purposes.

Studies of recent cases of damage to non-structural components, especially ceilings, has clarified some damage factors and led to some suggested measures to be taken for ceilings. However, understanding of and experimental evidence for the behavior of such complex-shaped ceilings is limited, so there is no well-established and appropriate seismic design method for them. A theoretical study on the static and dynamic behavior of the complex-shaped ceiling system is essential for appropriate ceiling design.

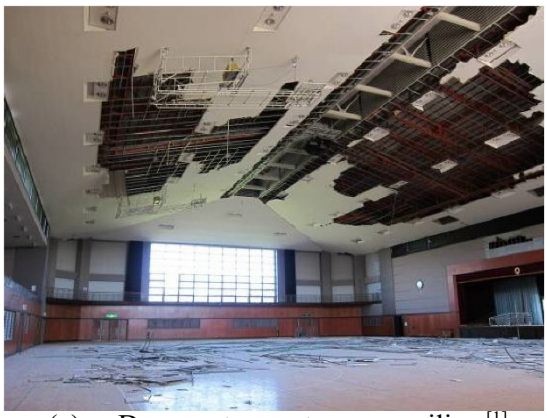

(a) – Damage to sports arena ceiling [1]

(b) – Damage to concert hall ceiling [2]

(c) – Damage to viewing hall ceiling [2]

Photos.1 – Damage to ceilings in the 2011 Off the Pacific Coast of Tohoku Earthquake

Since the 2011 disaster, certain measures have been mandated in Japan. However, there are few studies of seismic design for complex-shaped ceilings. Authors have tried to developed the seismic design method for them through the experimentation and previous knowledge. For the proper seismic design of ceilings with complex shapes, it is important to clarify the mechanical behavior. This paper focuses on the sloped ceiling as one of the various shapes.

In 2015, it has developed a seismic design for ceilings named the Linear Brace, see Fig. 1 and Fig. 2. The main feature of this method is that the gypsum board and structural elements are directly connected to the braces. Because of this, any inertial force is directly transmitted to the braces, rather than via elements such as connection pieces, furring brackets and furring strips. And the ceiling behavior is simple in the linear state with high stiffness. The authors have confirmed the mechanical properties of this method in static and dynamic experiments in reference [5] to [7] , and made it possible to design for flat ceilings with this mothod. After that, it have been continued experimental studies to apply the feature of Linear Brace to sloped eilings, and thought that simple design formulas described below in Section.2 can be used. However, in order to apply it to an actual sloped celing, it is necessary to verify that the the basic characteristics obtained through experimental research are appropriate in any cases. And, we thought that numerical varification using FEM analysis, the establishment of a seismic design method for sloped ceiling would advance dramatically. In the work reported here, as the first step, the characteristics of the sloped ceiling are verified numerically by FEM analysis and confirmed their consistency with experimental results.

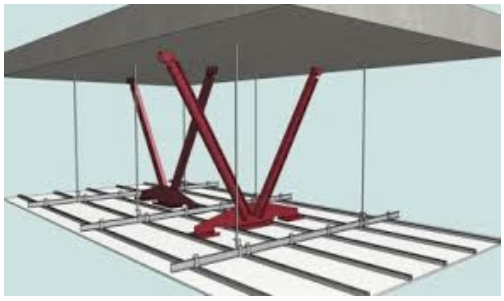

Fig. 1 – Configuration of new ceiling system [4]

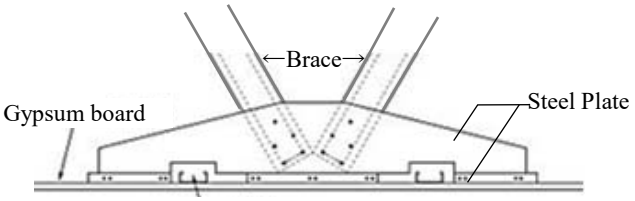

Fig. 2 – Joint for brace and gypsum board

2. Fundamental characteristics of sloped ceilings

A model of an angled ceiling with a θ_c degree inclination and composed of braces and suspension bolts is shown in Fig. 3(a). Next, we assume the replacement model as Fig. 3(b) in which the axial stress of suspension bolts N_{bolt} is replaced by reaction forces V_A and V_B because there is no vertical displacement ($\delta_A = \delta_B = 0$) at the suspension points, and the axial force N_{V1} and N_{V2} on brace are replaced by reaction forces F_x and Fz. Under horizontal loading P, to obtain F_x , F_z , V_A and V_B , the ceiling is replaced as a beam element, using Eq. (1) considering the bending moment term on a beam. Therefore, the external force "F" at the top of the V-brace in the plane of the ceiling is given by Eq. (2). The axial force on the brace is then described by Eq. (3), in which N_{V1} and N_{V2} are different. And the axial force on the suspension bolt is described by Eq. (4).

$$1 \cdot \delta_B = \int \frac{M\bar{M}}{E_c I_c} dx = 0 \tag{1}$$

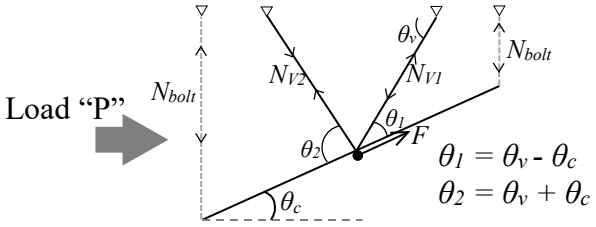

Fig. 3(a) – Basic model of proposed structure

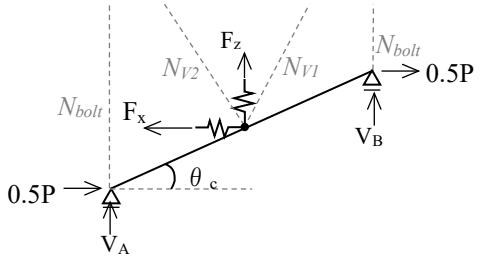

Fig. 3(b) –Simplified model

$$\text{External force: } F = P/\cos\theta_c \tag{2}$$

$$\text{Axial force on brace : } N_{V1} = \frac{\sin(\theta_2)}{\sin(\theta_1+\theta_2)} F \ , \ N_{V2} = -\frac{\sin(\theta_1)}{\sin(\theta_1+\theta_2)} F \tag{3}$$

$$\text{Axial force on suspension bolt: } \sum N_{bolt} = P \cdot \tan\theta_c \tag{4}$$

Looking at Eq. (4) we can see that suspension bolts will carry axial force which is tensile (+) under load "P" or compressive(-) under "-P". The suspension bolt, a threaded steel rod (W3/8) having a diameter of about 9 mm as generally used in Japan, can sufficiently resist tensile stress, but buckling will occur under a relatively small compressive stress.

With earthquake loading, which has a repeated positive and negative characteristic, there is a concern that the mechanical properties of the ceiling will differ under the positive and negative sides of loading due to the effect of buckling. If buckling is permitted, the assumed equilibrium state of the system in Eqs. (2) to (4) will not be maintained. To avoid this situation, we apply compression reinforcement to the suspension bolts, which avoids buckling and maintains the entire ceiling system in a stable state. Note that the suspension bolts described below are an element with sufficient resistance not only to tensile stress but also compressive stress. Therefore, in the following sections, the suspension bolt will be referred to as a reinforced hanging rod.

The validity of those characteristics has been confirmed through static and dynamic analysis and consistency with the experiments, in section 3 and 4.

3. Angle-dependent properties of sloped ceiling

The object of this section is to verify the behavioral characteristics of the sloped ceiling for angle dependance against horizontal static loads numerically by FEM analysis and to compare the consistency with static experimental results.

3.1 FEM model for static analysis

To examine behavior according to the degree of ceiling inclination, we executed a static analysis. Fig. 4 shows the Basic Constitution Model. The brace element V1 is on the upward side and element V2 is on the downward side of the slope. K_a is the joint stiffness between frame and brace. K_c is the joint stiffness between the brace and gypsum boad. Fig. 5 is the FEM model which is based on the Basic Constitution Model. The size of this model is 1,820mm x 3,640mm. The reinforced hanging rods are modeled with no-buckling.

Static analysis took place for ceiling angles of 10°, 20° and 30° up to ultimate loading. The applied load is defined as positive in the upward direction of the slope and as negative for downward.

Photo 2 shows the actual experimental setup which for comparing. In this experiment, hangingrods were reinforced for compression and not to buckle. The horizontal Y-displacement at the center of the ceiling was recorded.

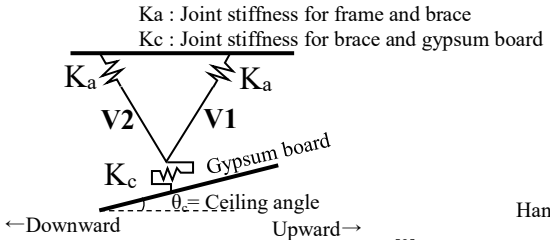

Fig. 4 – Basic constitution model[3]

Photo 2 – Static experiment setup

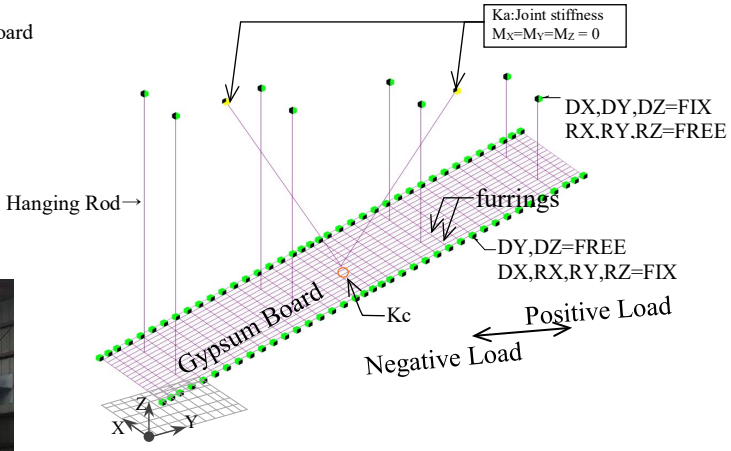

Fig. 5 – FEM model for static analysis

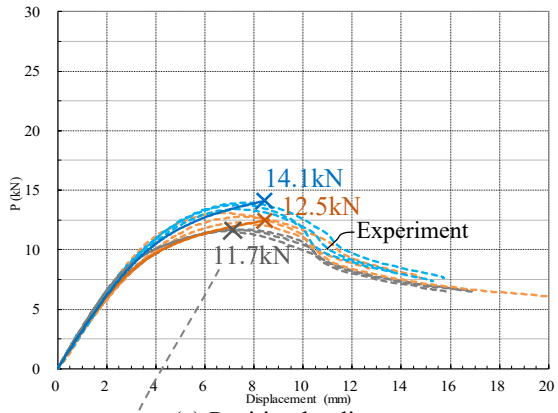

(a) Positive loading

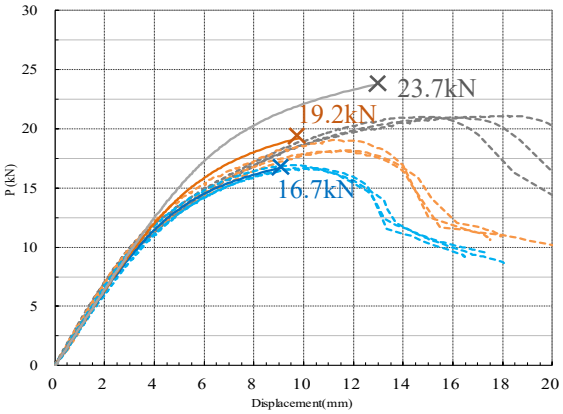

(b) Negative loading

Fig. 6 – Load-deformation curves

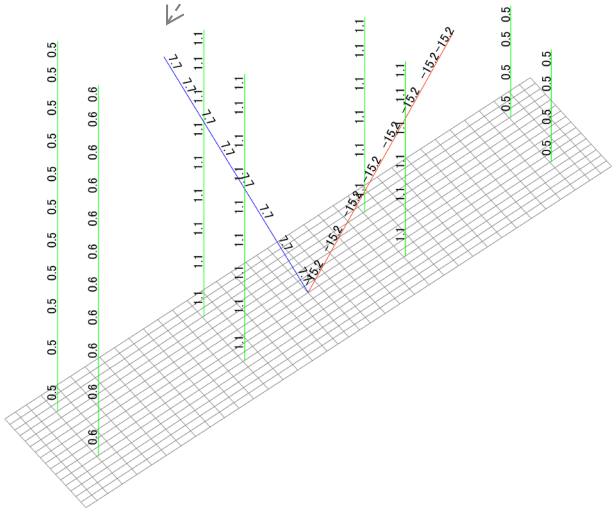

Fig. 7 –Axial stresses of braces and hanging rods under positive load P=11.7kN for θc=30° model

Table 1 – FEM results of maximum load for each angle

	Angle	θ_c=10°	θ_c=20°	θ_c=30°	Mode
Maximum load(kN)	$P_{max}(+)$	14.1	12.5	11.7	Buckling of brace element V_2
	$P_{max}(-)$	16.7	19.2	23.7	Buckling of brace element V_1
$P_{max}(-) / P_{max}(+)$		1.18	1.54	2.0	-
$\sin\theta_1/\sin\theta_2$		1.22	1.53	2.0	-

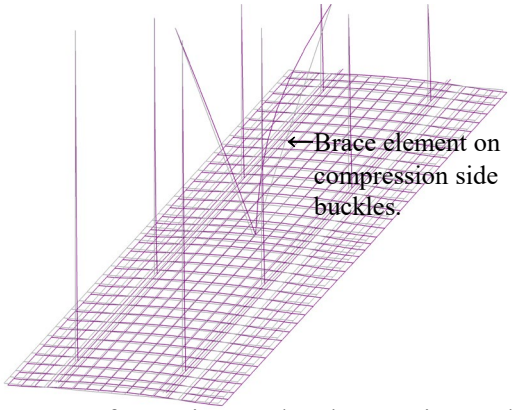

Fig. 8 – Deformation under the maximum load

Table 2 – Comparison of axial stress between FEM and calculation

	Brace			Hanging rods
	axial force (kN)		N_{V1}/N_{V2}	axial force (kN)
	N_{V1}	N_{V2}		Total
FEM	15.2	7.7	1.97	6.5
Calculated	15.6	7.8	2.00	6.7

Fig. 6(a) and 6(b) show the relationship between horizontal load and Y-displacement on center point of the ceiling surface as solid lines. In this analysis, the maximum load (=P_{max}) is defined as the load step at just before when the stiffness falls below 1/10 of the initial stiffness or at a solutions can be unstable.
Fig. 6(a) is under positive loading and Fig. 6(b) is under negative loading. The grey curves represent θ_c=10°, orange θ_c=20°, and blue θ_c=30°. For comparison, experimental results are shown by the dashed lines, with three experimental cases per angle. The results of FEM analysis and experiment are generally consistent. Table 1 lists the maximum load for each angle and force direction.
Fig. 7 shows the axial stress diagram of brace and hanging rods at the incremental load equal to 11.7kN in Fig. 6(a), taking ceiling angle θc = 30° as an example. The axial stresses carried by the V-bracing under a

horizontal load of 11.7 kN are N_{V1} = 15.2 kN on the compression side and N_{V2} = 7.7 kN on the tension side. From Table 2, FEM analysis results are seen to be consistently accurate as compared with calculated values obtained using Eqs. (2) and (3), although there are a little nonlinearity before reaching the maximum load in Fig.6(a).
And, as is clear from Fig. 7, each rod element is subject to an axial stress. The sum of the axial forces carried by the surrounding hanging rods can be expressed by P · tan θc (= Eq. (3)) (see Table 2).

Regarding the maximum strength of the ceiling, the following conclusions can be drawn from Figs. 6(a), 6(b) and Table 1:
(i) Under positive loading, the maximum load is higher at a smaller inclination. On the other hand, under negative loading, the maximum load is higher at a greater inclination.
(ii) For a given sloped ceiling angle, the ratio of negative load to positive load varies from 1.2 to 2.0 at different angles.
From (i) and (ii), it is clear that the maximum strength of the sloped ceiling depends on the ceiling angle θc, and the direction of loading. In these results, since the mode of collapse was buckling of the braces on the compression side in all load cases, axial stress of brace determine the strength. The ratio of strength P (-) / P (+) equals $\sin\theta_1$ / $\sin\theta_2$, which is expressed with high accuracy by using Eq. (3). In this experiment, no buckling of the reinforced hanging rods was observed even under negative loading.

In this section, it is confirmed that the axial stresses carried by not only braces but also hanging rods, and those value can be expressed accurately by Eqs.(3) and (4).

4. Dynamic properties

The aim of this dynamic analysis is to confirm the response properties of the proposed ceiling, namely acceleration of the ceiling surface and axial stresses on the braces and hanging rods.

4.1 FEM model for dynamic analysis

Fig. 9 shows the FEM model which has ceiling angle θc = 20°. This model comprises 2 braces(C-40x20x10x1.6, C-65x30x10x1.6), 8 hanging rods and gypsum board(25mm). And supporting flame(H-350x175x7x11) is modeled. Stiffness is applied as in section 3, Ka to frame and brace joints and Kc to brace and gypsum board joints.
The mass of the ceiling is about 140kg (20kg/m^2 x 1.82m x 3.64m/cos20°) and the input acceleration applied by the shaking table is about 12.65m/s^2. Therefore, the inertial force on the ceiling surface is about 1,771N.

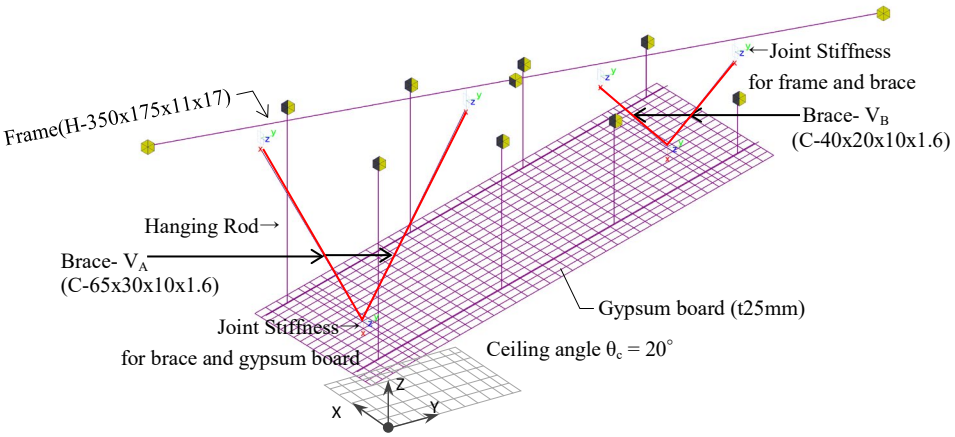

Fig. 9 – FEM model for dynamic analysis

To compare, we refer to a dynamic experiment. Photo 3 shows the experimental setup for dynamic testing of the model with the same specifications as FEM model. Acceleration was recorded at three points (A to C) on the gypsum-board and strains of braces and hanging rods were measured (see Fig. 10).

Photo 3 – Dynamic experiment setup

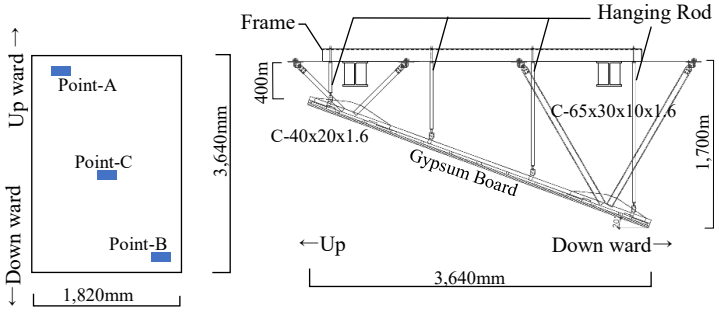

(a) Plan (b) Elevation

Fig. 10 – Schematic of dynamic experiment

4.2 Coordinate definition

For this section, we define global coordinates in which the X, Y and Z axes align with the frame and local coordinates in which the axes x_c, y_c and z_c are defined with respect to the ceiling surface (see Fig. 11).

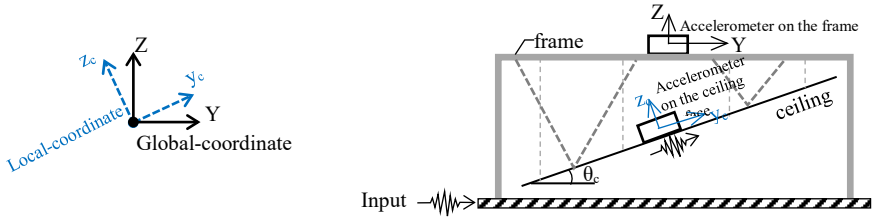

Fig. 11 – Coordinate definition

4.3 Vibration mode

Fig. 12 gives the mode shape diagrams as obtained by FEM analysis. Fig. 13 shows the experimental transfer functions (acceleration at three points on ceiling to acceleration on frame) under white-noise excitation. Their directions indicate y_c / Y and z_c / Z. From Peak- y_c / Y in Fig. 13(a) and the mode shape in Fig. 12(a), the natural frequency in Y-axis vibration of the whole ceiling unit is found to be around 32Hz. Peak- z_c / Z in Fig. 13(b) and the mode shape in Fig. 12(b) indicate the out-of-plane vibration of the gypsum panels which of the natural frequency in Z-axis is found to be around 17Hz. Note that due to the experimental size limitation, natural frequency of Y-axis is higher than general, and that of Z-axis is lower than general. These are the two main vibration modes in this experimental model.

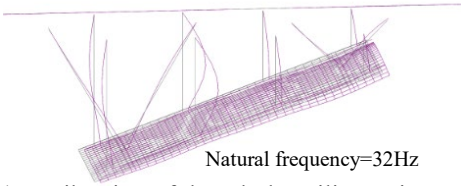

(a) Y-vibration of the whole ceiling unit

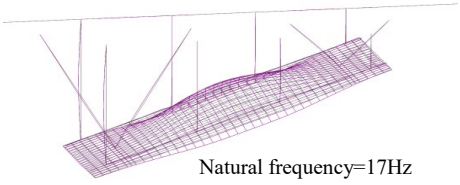

(b) Out-of-plane vibration

Fig. 12 – Natural frequency by FEM analysis

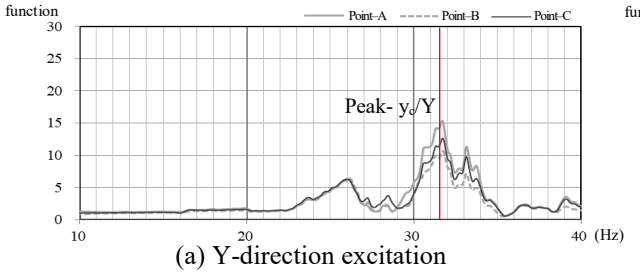

(a) Y-direction excitation

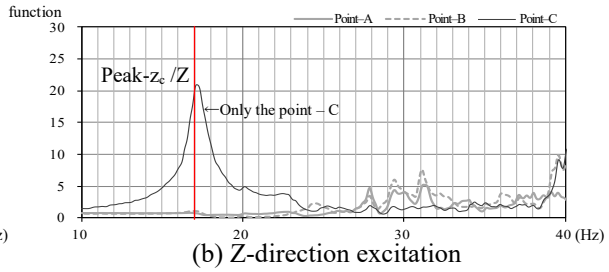

(b) Z-direction excitation

Fig. 13 – Transfer function of experimental

4.4 Response to dynamic load

In this dynamic experiment, the input acceleration is a 3 Hz sine wave in the direction of the Y-axis and the maximum acceleration is 1,265 cm/s^2 (see Fig. 14). Here, time history results by FEM analysis are expressed as a continuous line. And to compare, the referenced experimental results are expressed by a dashed line.

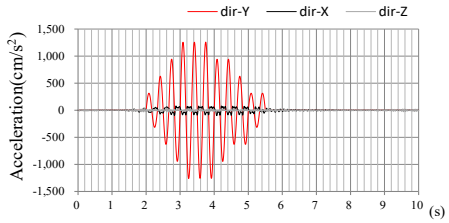

Fig. 14 – Time-history of input acceleration

Table 4—Comparison of calculated values and the maximum acceleration response

		Maximum acceleration (cm/s^2)		
predicted	y_c	1,178		
	z_c	489		
		Point-A	Point-B	Point-C
FEM analysis	y_c	1,223	1,223	1,223
	z_c	434	449	900
Experimental	y_c	1,191	1,191	1,215
	z_c	536	536	768

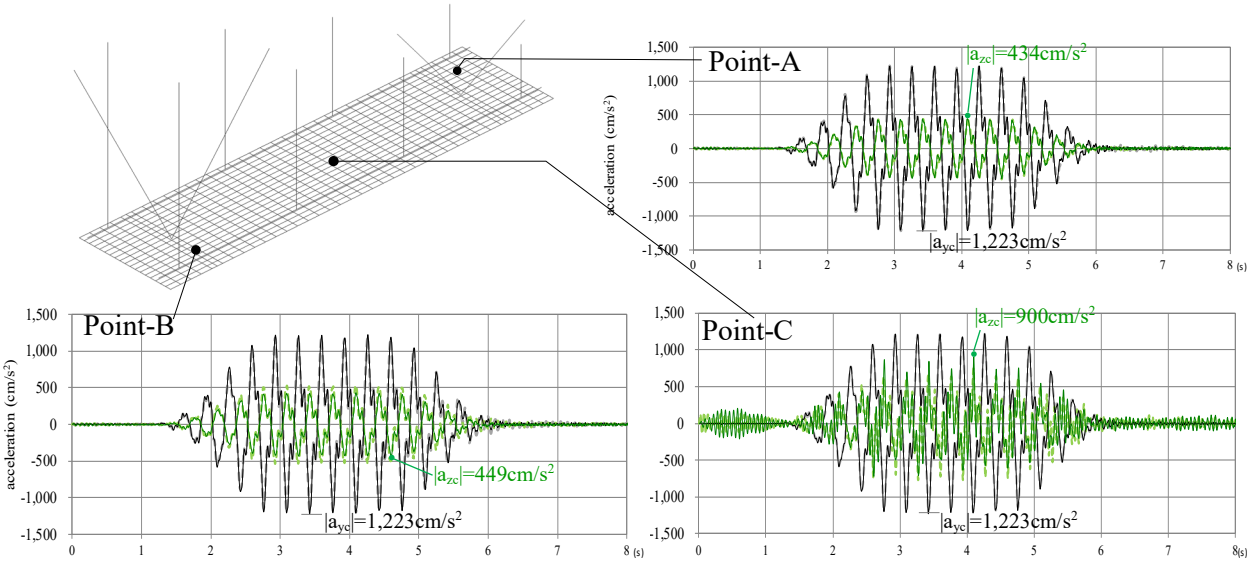

Fig. 15 – Time histories of acceleration on the ceiling surface

i) Response acceleration on the ceiling surface

Fig. 15 shows the time-history acceleration response at points A, B and C on the ceiling surface. The black line is the acceleration in the y_c-axis direction, which is in-plane with the ceiling board, and the green line is in the z_c-axis direction, which is out-of-plane. This demonstrates that dynamic horizontal loading causes acceleration in the both y_c and z_c directions, so it has an influence on both horizontal and vertical response. Table 4 is a list of maximum accelerations obtained by FEM analysis and predicted by Eq. (5), and experimental results for comparison. Eq. (5) is based on Eq. (2) and (4) with a transformation into the local coordinates shown in Fig. 10. The predicted acceleration on the gypsum board in the y_c-axis approximates to the results of FEM analysis and to the experimental results at all points. In the z_c-axis, the response at points A and B approximates to the predicted value. On the other hand, the result at point C, which is in the center of the model, is 2 times greater than at other recorded points. This is out-of-plane amplification of the gypsum board, which is the mode shown in Fig. 13(b). The reason for this amplification is the fulcrum distance (1.4m) of the hanging rod, which was too long. After setting it to the proper distance, which is 0.9m, the amplification rate is not so large.

$$a_{yc} = a_g \times ((1 - \sin^2\theta_c)/\cos\theta_c) \quad , \quad a_{zc} = a_g \times \sin\theta_c \qquad \text{Eq.(5)}$$

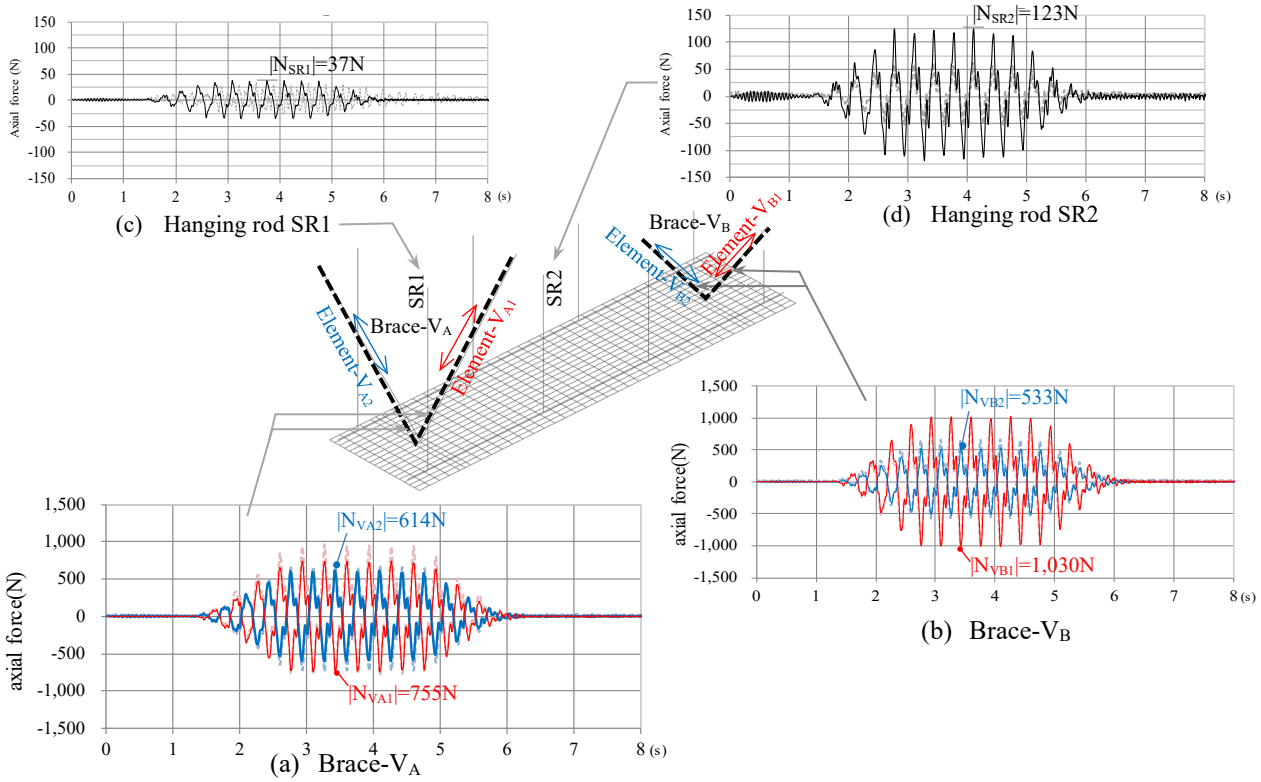

Fig. 16 – Time histories of axial forces on braces V_A and V_B, and hanging rods SR1 and SR2

Table 5—Comparison of brace axial forces

Unit:(N)

	Brace-V_A		Brace-V_B	
	N_{VA1}	N_{VA2}	N_{VB1}	N_{VB2}
Calculated	714	467	1,138	530
FEM analysis	755	614	1,030	533
Experimental	826	649	970	643

Table 6—Comparison of hanging rod axial forces

Unit:(N)

	SR1	SR2	SR3	SR4	Total
Calculated	-				322
FEM analysis	37	126	136	34	333
Experimental	30	59	51	33	173→398*

ii) Axial force of braces

Fig.16(a) and (b) are time-histories of the axial force response of brace V_A and brace V_B. The red line indicates elements V_{A1} and elements V_{B1}, which are on the upper side. The blue line indicates elements V_{A2} and elements V_{B2} which are on the lower side. The two responses are quite different, with the axial force value N_{VA1} on element V_{A1} typically about 1.2 times larger than N_{VA2} on element V_{A2}. All values of maximum axial force for the braces are shown in Table 5. When the load distribution on the two sets of braces is apportioned in accordance with the stiffness ratio, the value of the axial force in each element calculated from Eq. (3) is an accurate prediction of the experimental value, except in the case of N_{VA2}. The experimental values are estimated using ε x E x A.

Specifications of Braces are below.

The Young's modulus E is 205,000N/mm^2. Areas A which except lip are 183mm^2 (V_A) and 111mm^2 (V_B).

iii) Axial force of hanging rods

Fig. 16(c) and (d) show the time-histories of the axial force response of hanging rods SR1 and SR2. The values were estimated using ε x E x A. All values of maximum axial force for the hanging rods are shown in Table 6. The total maximum axial force is approximately 173N. In this experiment, the measured strain is of the reinforcing element only, so the relationship between reinforcing element and bolt must be taken into

account. This means that the ($E_sA_s + E_pA_p$) / E_pA_p ,total axial force is about 2.3 times 173N, then 398N is estimated. The total axial force in the hanging rods as calculated from Eq. (4) is an accurate prediction of the experimental value.
Specifications of Hanging rod are below.
Iner bolt (W3/8) : E_s=205,000N/mm^2 , A_s=63mm^2. Reinforcing element : E_p=69,000N/mm^2 , A_p=143mm^2

5. Conclusion

In this paper, it is verified the main resistance mechanism of a sloped ceiling against horizontal load by numerical analysis and confirmed the consistency of the numberical results against static and dynamic experiments. And simple formulas(Eqs.(1) to (4)) for seismic design of sloped ceilings were validated. The results obtained can be summarized as follows.

#1 When a horizontal load is applied to a sloped ceiling, the resistance elements are the braces and hanging rods under axial stress. It is possible to accurately express these axial stress using Eqs. (2) to (4). They are depend on the ceiling angle θ_c and loading direction.

#2 When a dynamic horizontal load is applied to a sloped ceiling, there are two main vibration modes, in-plane and out-of-plane. The out-of-plane ratio is approximately the input acceleration times sinθc accoding to the ceiling angle, and it can not be ignored.

#3 In this study, an effective means of obtaining stable behavior is to turn the suspension bolt (W3/8) into a hanging rod by providing reinforcement against compressive axial stress under earthquake loading.

The method reported in this paper allows us to predict approximate response values for an angled ceiling suspended below a flat horizontal structure. It does not cover the behavior of a ceiling when the structure itself is inclined. This is a future work for the authors.

6. Acknowledgements

This work was supported by JST Program on Open Innovation Platform with Enterprises(JPMJOP1723), Research Institute and Academia (OPERA). The authors gratefully acknowledge the implementation of the static experiment and some materials tests by SOMENO Factory Co., Ltd.

7. Reference

[1] National Institute for Land and Infrastructure Management(NILIM) (2011): Summary of the Field Survey and Research on “The 2011 off the Pacific coast of Tohoku Earthquake”, Technical Note of National Institute for Land and Infrastructure Management, No.647, 09/2011, Japan

[2] Yoshio WAKIYAMA, Tadashi ISHIHARA, Shojiro MOTOYUI, Tsuyoshi SEIKE, Isao SAKAMOTO, Sachi OHMIYA, Yusuke OKI, (2019): A Study on the Establishment of Standards of Suspended Ceilings Based on Seismic Damage from the Great East Japan Earthquake, Building Research Institute(BRI), Building Research Data No.193,03/2019, Japan

[3] NILIM, BRI (2013) : *Practical Guide on the Technical Standards concerning Measures to Prevent the Fall of Ceilings in Buildings*, Technical Note of NILIM No.751, Building Research Data No.146, September 2013

[4] SHIMIZU CORPORATION, “Linear Brace”, 03/2016, https://www.shimz.co.jp/company/about/news-release/2016/2015064.html, in Japanese

[5] Kenji Suzuki, Fumihiko Sakuraba, Tetsuya Hanzawa (2017): DEVELOPMENT OF “DIRECT & LINEAR BRACE SYSTEM OF CEILINGS”, *AIJ Journal of Technology and Design, vol.23*, 2/2017, pp.153-158

[6] Fumihiko Sakuraba, Kenji Suzuki, Tetsuya Hanzawa, Mika kaneko (2015): Development of “Direct & Linear Brace system of Ceilings” Outline of development and Lateral loading test. *AIJ 05/2015,* pp.825-826

[7] Kenji Suzuki, Fumihiko Sakuraba, Tetsuya Hanzawa, Mika kaneko (2015): Development of “Direct & Linear Brace system of Ceilings” Outline of development and Lateral loading test. *AIJ 05/2015,* pp.827-828

